Electronic Supplementary Material (ESI) for Sustainable Energy & Fuels.

Electronic Supplementary Information

Controllable construction of oxygen vacancies by anaerobic catalytic combustion of dichloromethane over metal oxides for enhanced solar-to-hydrogen conversion

Sufen Zhang, Jianni Liu, Xiaoyang Dong, Xiaoxia Jia, Ziwei Gao, and Quan Gu*

Key Laboratory of Applied Surface and Colloid Chemistry, Ministry of Education, School of Chemistry and Chemical Engineering, Shaanxi Normal University, Xi'an, 710062, China

*E-mail: guquan@snnu.edu.cn

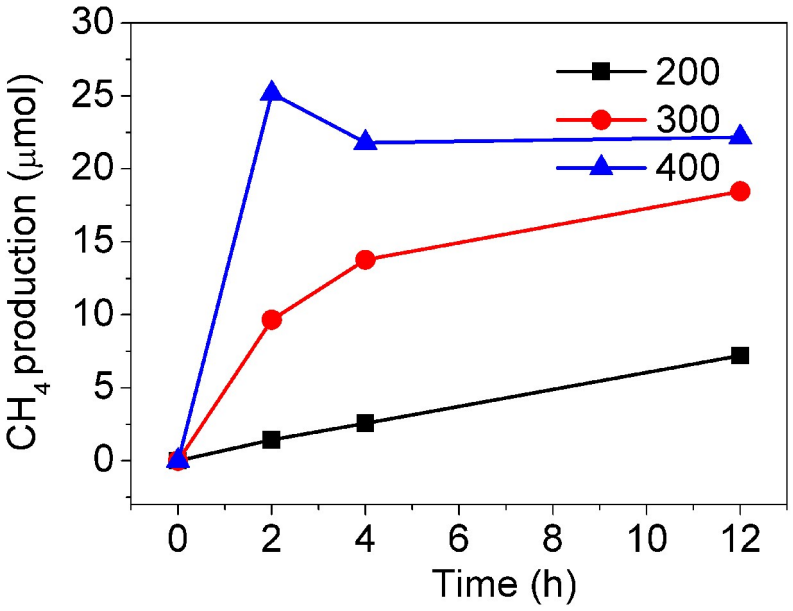

Figure S1 amount of CH_4 detected by GC during the reaction of CH_2Cl_2 with TiO_2 at 200, 300, and 400 ^oC.

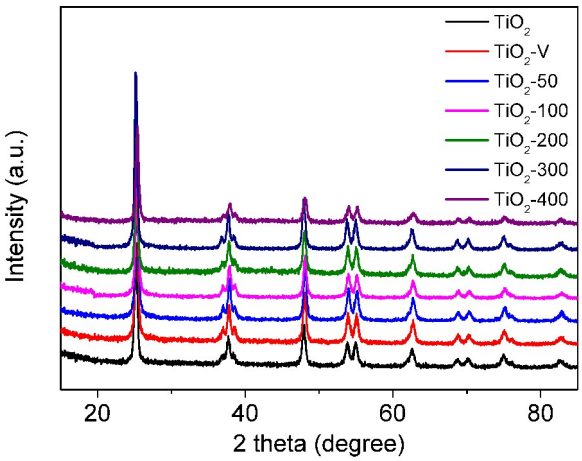

Figure S2 XRD patterns of TiO_2, TiO_2-V, and TiO_2-T (T=50, 100, 200, 300, and 400).

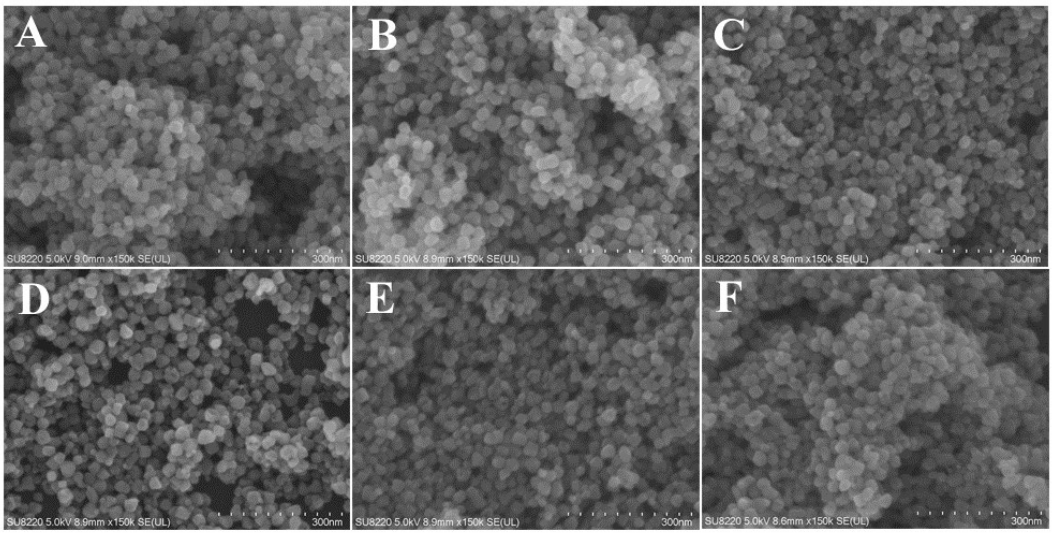

Figure S3 SEM images of TiO_2 (A), TiO_2-50 (B), TiO_2-100 (C), TiO_2-200 (D), TiO_2-300 (E), and TiO_2-400 (F).

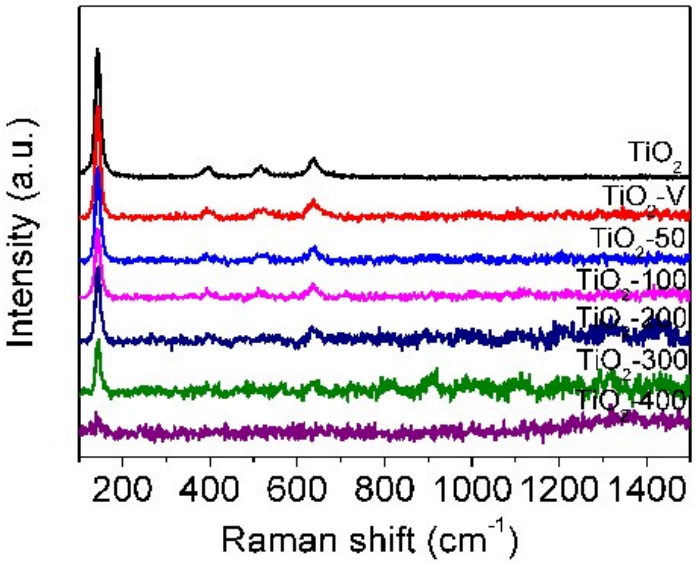

Figure S4 Raman spectra of TiO_2, TiO_2-V, and TiO_2-T (T=50, 100, 200, 300, and 400) obtained at different reaction temperature.

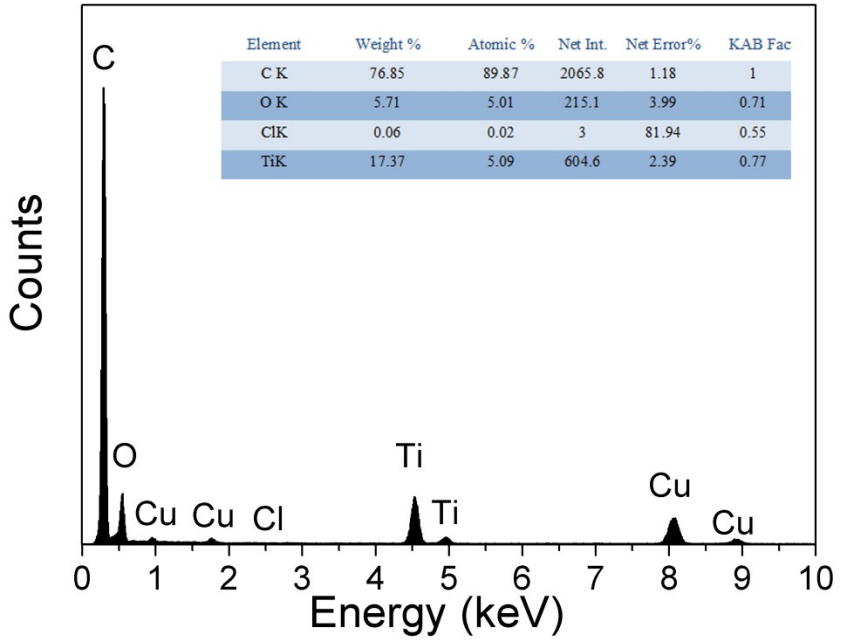

Figure S5 EDX image of TiO_2-200.

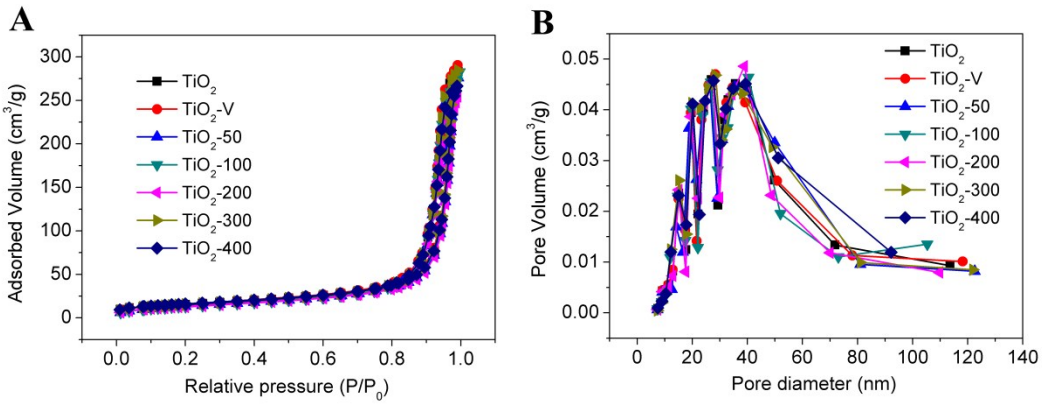

Figure S6 the nitrogen adsorption-desorption isotherms (A) and the corresponding pore-size distribution curves (B) of TiO_2 and TiO_2-T (T=50, 100, 200, 300, and 400) obtained at different reaction temperature.

Table S1 summary of the physicochemical characteristics of as-prepared samples.

sample	Pore volume (ml/g)	Pore size (nm)	S_{BET} (m^2/g)
TiO_2	0.5385	26.46	55.3
TiO_2-V	0.4499	25.95	56.9
TiO_2-50	0.4272	26.49	51.3
TiO_2-100	0.4250	26.31	51.5
TiO_2-200	0.3938	25.96	49.5
TiO_2-300	0.4408	25.99	57.3
TiO_2-400	0.4127	25.81	57.6

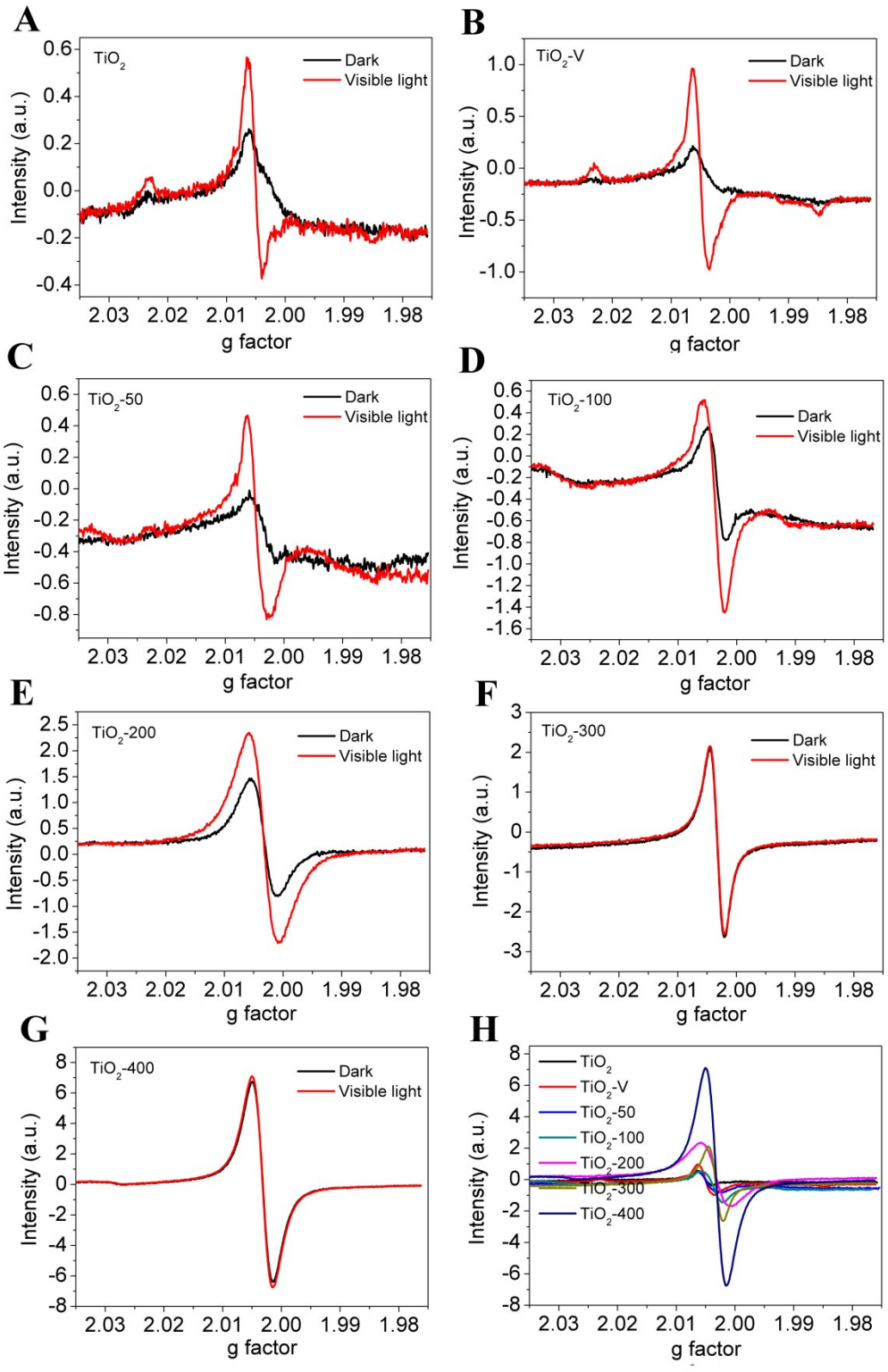

Figure S7 EPR spectra of TiO_2, TiO_2-V, and TiO_2-T (T=50, 100, 200, 300, and 400) obtained at different reaction temperature determined at 140 K under dark and visible light irradiation.

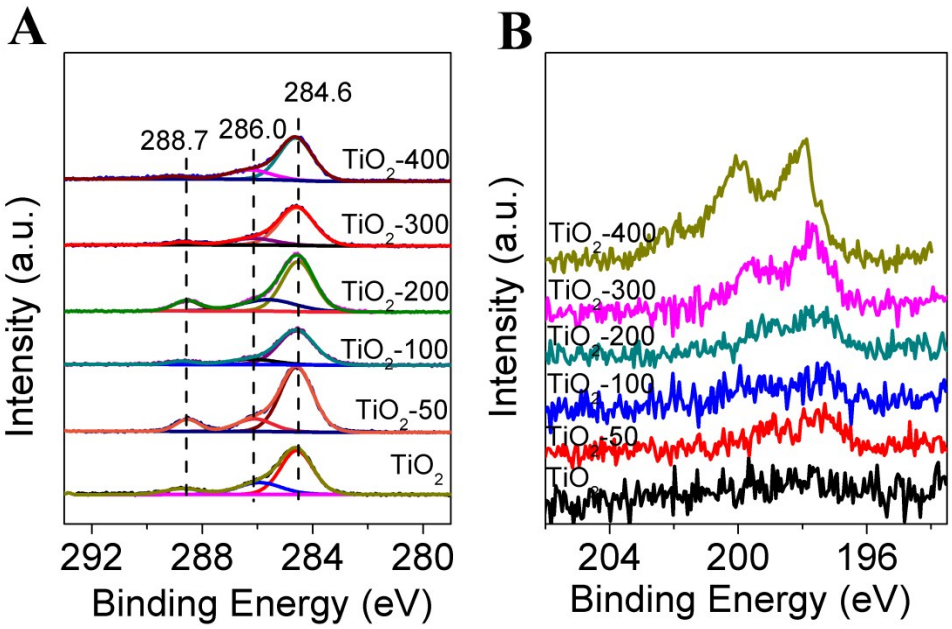

Figure S8 high-resolution C 1s and Cl 2p XPS spectra of TiO_2 and TiO_2-T (T=50, 100, 200, 300, and 400) obtained at different reaction temperature.

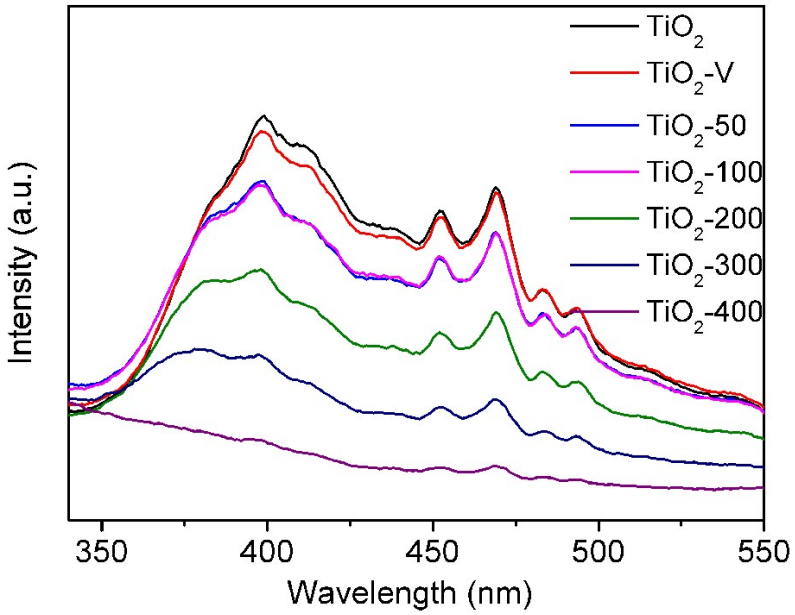

Figure S9 PL spectra of TiO_2, TiO_2-V, and TiO_2-T (T=50, 100, 200, 300, and 400) obtained at different reaction temperature.

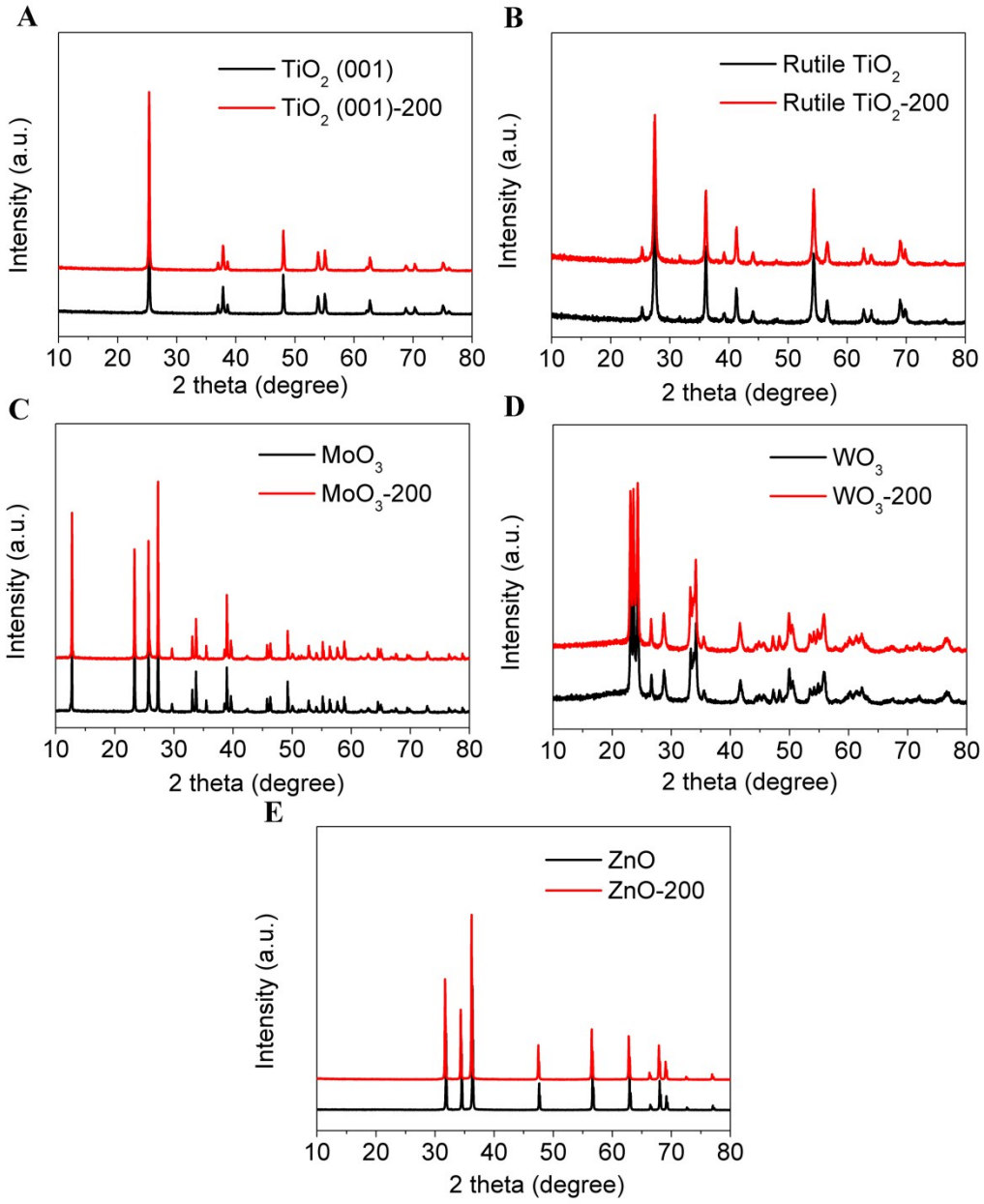

Figure S10 XRD patterns of (A) TiO_2 (001), (B) rutile TiO_2, (C) MoO_3, (D) WO_3, and (E) ZnO before and after treatment.

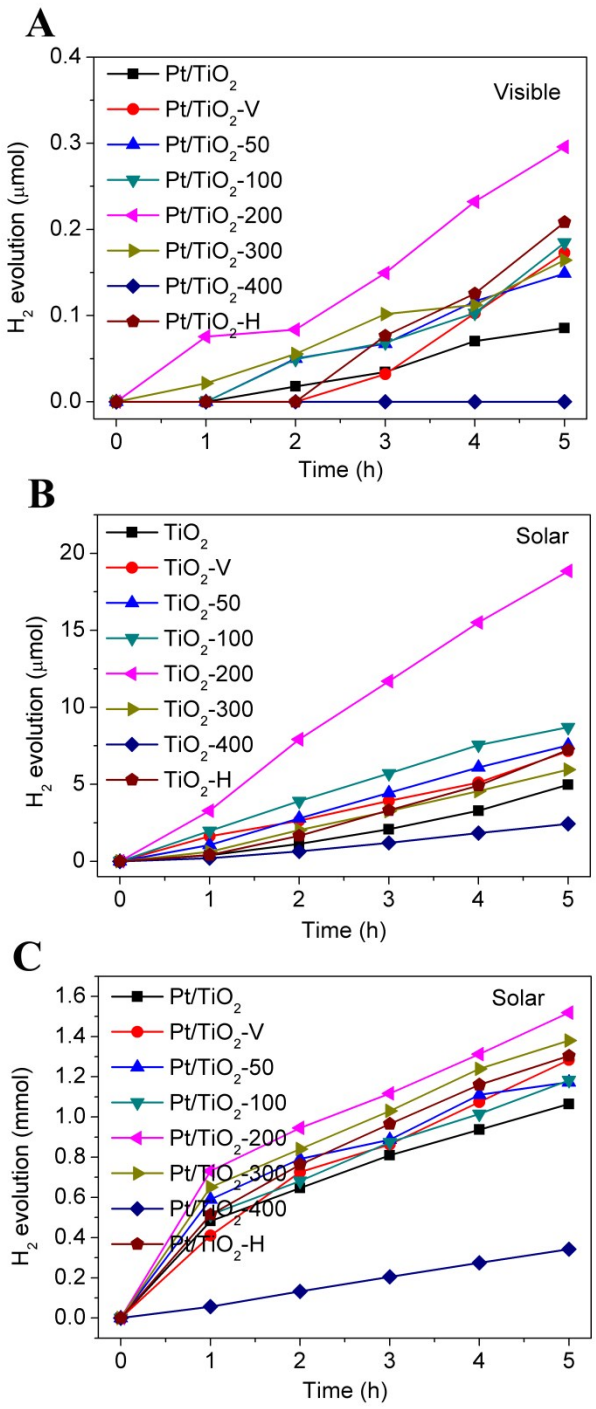

Figure S11 (A) Hydrogen evolution amount of Pt supported samples from ethanol solution (10 vol%) under visible light irradiation. (B) Hydrogen evolution amount of TiO_2, TiO_2-T (T=50, 100, 200, 300, and 400) obtained at different reaction temperature, TiO_2-V, and TiO_2-H from ethanol solution (10 vol%) solar light irradiation. (C) Hydrogen evolution amount of Pt supported samples from ethanol solution (10 vol%) under solar light irradiation.

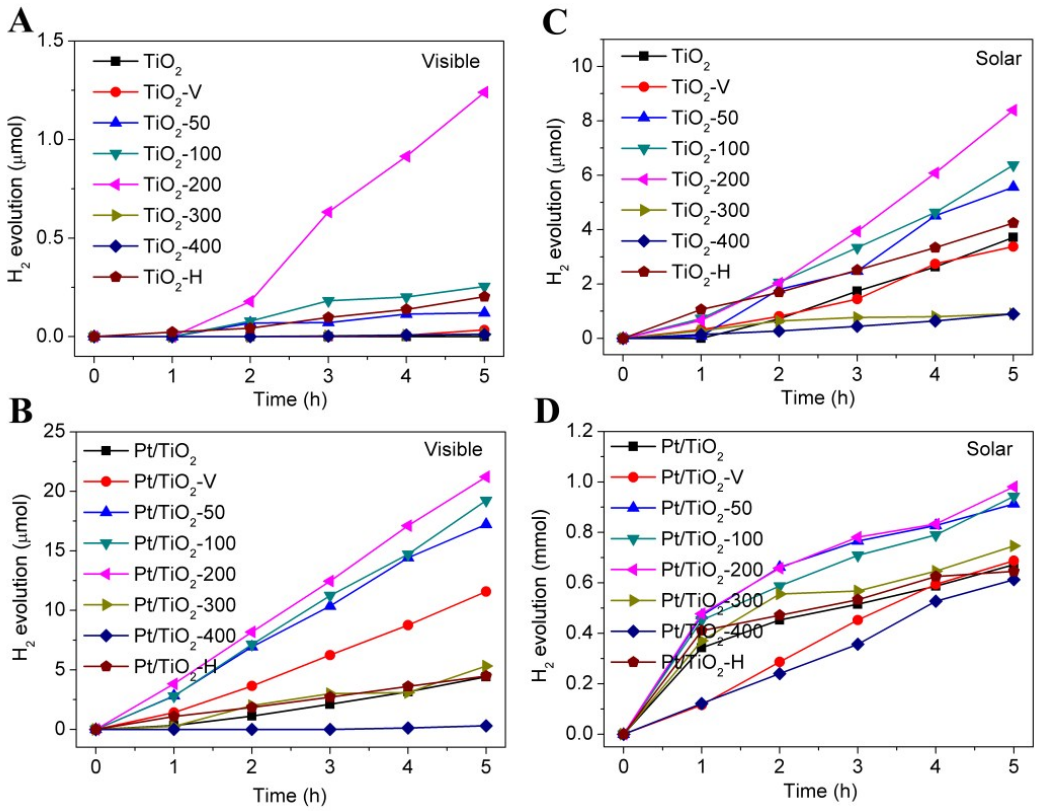

Figure S12 hydrogen evolution amount of (A) TiO_2, TiO_2-T (T=50, 100, 200, 300, and 400) obtained at different reaction temperature, TiO_2-V and TiO_2-H and (B) the corresponding Pt supported samples from EDTA-2Na solution (1.0 mg/ml) under visible light irradiation. Hydrogen evolution amount of (C) TiO_2, TiO_2-T (T=50, 100, 200, 300, and 400) obtained at different reaction temperature, TiO_2-V and TiO_2-H and (D) the corresponding Pt supported samples from EDTA-2Na solution (1.0 mg/ml) under solar light irradiation.

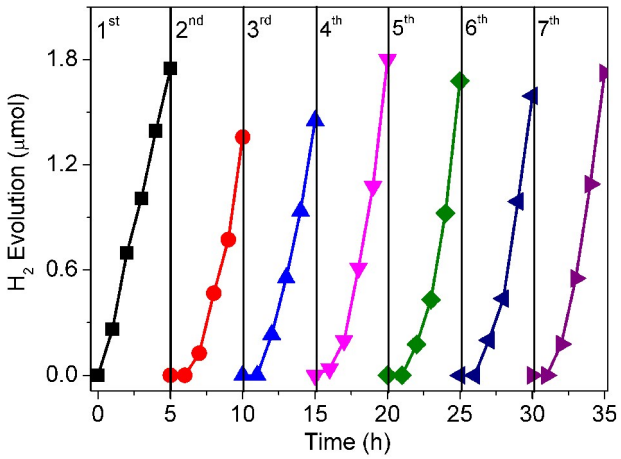

Figure S13 cycling test of TiO_2-200 for photocatalytic H_2 generation form EDTA-2Na solution under visible light irradiation (λ>420 nm).

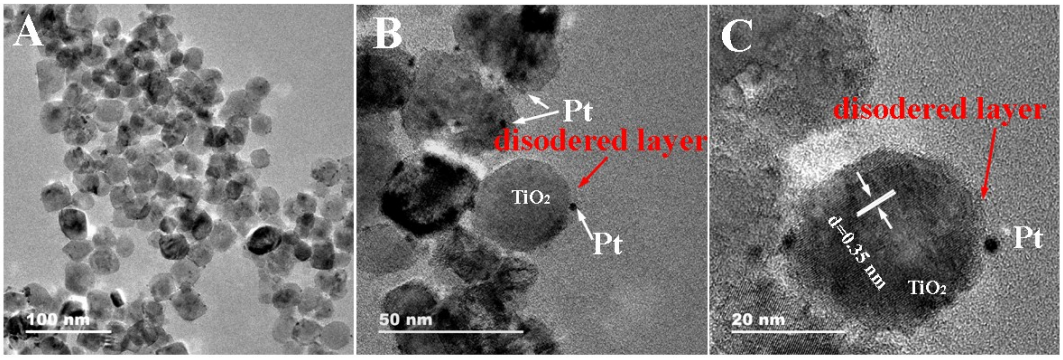

Figure S14 TEM (A and B) and HRTEM (C) images of Pt nanoparticles supported TiO_2-200.